**Journal of Sciences, Islamic Republic of Iran 20(3): 243-251 (2009)** http://jsciences.ut.ac.ir
University of Tehran, ISSN 1016-1104

# Magmatic Interaction as Recorded in Texture and Composition of Plagioclase Phenocrysts from the Sirjan Area, Urumieh-Dokhtar Magmatic Arc, Iran

B. Monfaredi,[1,*] F. Masoudi,[1,2] A.A. Tabbakh Shabani,[3]
F. Shaker Ardakani,[1] and R. Halama[4]

[1]*Department of Geology, Tarbiat Moallem University, Tehran, Islamic Republic of Iran*
[2]*Factuality of Earth Science, Shahid Beheshti University, Tehran, Islamic Republic of Iran*
[3]*Research Center for Earth Sciences, Geological Survey of Iran, Tehran, Islamic Republic of Iran*
[4]*Institut Für Geowissenschaften, Universität Kiel, 24118 Kiel, Germany*

Received: 21 June 2009 / Revised: 14 September 2009 / Accepted: 30 September 2009

## Abstract

Tertiary andesitic basalts of the Sirjan area, Urmieh-Dokhtar Magmatic Arc, Iran, contain plagioclase phenocrysts enclosed in a matrix of amphibole, clinopyroxene and rare olivine crystals. Textural and compositional evidence suggests two significantly different types of plagioclase phenocrysts occur in the andesitic basalts. The most common type of plagioclase phenocrysts have zoning patterns that display abrupt fluctuations in An content (more than 20 mol %) that correspond to well-developed dissolution surfaces. The less common type of plagioclase phenocrysts is characterised by a core with sieve texture, which is overgrown by oscillatory zoned rims. Changes in temperature, composition and $H_2O$ content of the surrounding melt caused the development of resorption zones in the engulfed plagioclases. In addition to the petrographical and mineral chemical evidences, Crystal Size Distribution (CSD) measurements show a kinked plot that reflects the effects of degassing and reveals mixing of two different phases of nucleation and growth. It is assumed that plagioclase phenocrysts originally crystallizing from the host magma were interrupted by mixing with a volatile-rich magma possessing low phenocryst content. The gradual loss of volatiles from plagioclase-saturated intrusive magma could be responsible for the sieve-textured core.

**Keywords:** CSD; Sieve texture plagioclase; Mixing; Resorption; Sirjan; Iran

## Introduction

Igneous rocks develop from the crystallisation of magmas by a complex interplay of crystal nucleation and growth. This makes interpretation of magmatic processes complicated. To obtain a more extensive comprehension of the magmatic processes, petrologic studies prevalently utilize a combination of compo-

* Corresponding author, Tel.: +98(21)88309293, Fax: +98(21)88309293, E-mail: monfaredi.b@gmail.com

sitional data and textural characteristics of individual phenocrysts [e.g. 27, 8, 25, 6, 12].

Chemical and textural zoning patterns in plagioclase phenocrysts comprise valuable information for instance, changing melt-crystal compositions, and describe how magmas of differing compositions and physical properties chemically interact in the chamber. Compositional and textural information recorded in plagioclase from volcanic rocks have been studied by many researchers to investigate different aspects of magma chamber dynamics [e.g. 23,24,16,27,28,29,10,9,25,6]. This is because plagioclase, an extremely common tectosilicate mineral in many types of igneous rocks, crystallizes over a large range of temperatures.

The major compositional changes of plagioclase are related to a variety of parameters such as melt composition, $H_2O$ content, temperature and pressure [e.g. 7, 13, 16, 27], decompression [22], and growth rate [15]. Thus, it is difficult to differentiate which parameters are the most important to cause compositional variations in any particular case and which main events might have occurred in a magma chamber.

Most recently it has been shown that Crystal Size Distributions (CSDs) study provides information on the crystallisation history of a magma chamber and the textural evolution of igneous systems as preserved in the solid rock [e.g. 18,1,11,20,2,12]. The CSD method has been used to establish whether magma solidification occurred as a result of a single crystallization system or two different crystallization ones [18,11,12]. In addition, CSD studies have been applied to provide information on crystal growth rate and residence time of crystals in the liquid [18], nucleation density and magmatic processes such as crystal accumulation and fractional crystallisation [18,12], and coarsening (Ostwald ripening, textural equilibration) [e.g. 18,12]. Furthermore, CSD studies have been used to identify distinct episodes of magma ascent, storage and quenching with no relationship with mixing of different populations [1].

In this study, we report major compositional changes in plagioclase phenocrysts from basaltic andesite of the Sirjan area in Iran. We interpret these changes as response to the changes in temperature and water content and composition of the surrounding melt in the calc-alkaline magma. The plagioclase crystals become partially resorbed due to complicated processes involving mixing events. The CSD results reveal a kinked pattern in the crystal population interpreted as a mixed population of crystals which indicate that crystals might have originated from two different magmas.

### *Geological Overview*

Subduction of Tethyan oceanic lithosphere under the southwestern border of Central Iran triggered plutonic and volcanic activities between the Jurassic and Quaternary in a NW-SE trending zone called Urmieh-Dokhtar Magmatic Arc (UDMA) (Fig. 1) [26, 5, 4, 21]. Magmatic activities in the UDMA with a length of approximately 1700 km and a width of 100 km occurred mainly in the Tertiary as result of the above mentioned subduction. The lavas and pyroclastic rocks are alkaline and calc-alkaline, ranging from basalt and andesitic basalt to dacite and trachyte (Fig. 1) [5].

Andesitic basalt of the Sirjan area is part of the numerous volcanic rocks in the UDMA, located between 29° 38′ 43″ and 29° 41′ 44″ latitude and 56° 08′ 00″ to 56° 12′ 00″ longitude in the northwest of Kerman province, SE Iran (Fig. 1). The rock occurs mainly as massive flows and has a blocky outcrop. For the purpose of this study, various samples were studied and only a sample selected as a representative for electron probe microanalysis (EPMA) and CSD studies. This sample is porphyritic, in which the large subhedral to euhedral crystals referred to as phenocrysts are plagioclase dispersed in a matrix of accessory minerals such as clinopyroxene, olivine, amphibole, glass opaque and altered minerals like chlorite, epidote and serpentine.

## Materials and Methods

### *Electron Microprobe Measurements*

Composition of the plagioclase crystals was determined using CAMECA SX-100 electron microprobe of Iran Mineral Processing Research Center. Mineral analyses were conducted using a 5 μm beam diameter and an accelerating voltage of 15 kV and a beam current of 10 nA. 9 to 11 point analyses were carried out in a mode of rim-core-rim traverses based on are as follow: the zoned plagioclase back scattered electron image (BSE). The results are shown in Table 1.

Natural standard samples which were used for EPMA calibration albeit for Na, diopside for Mg, corundum for Al, wollastonite for Si and Ca, orthoclase for K, rutile for Ti and hematite for Fe.

### *Crystal Size Distribution Analyses*

The representative sample was analyzed to characterize the effects of crystal growth during cooling.

In a steady-state open system a “simple” crystallization history is preserved as a log-linear CSD, where

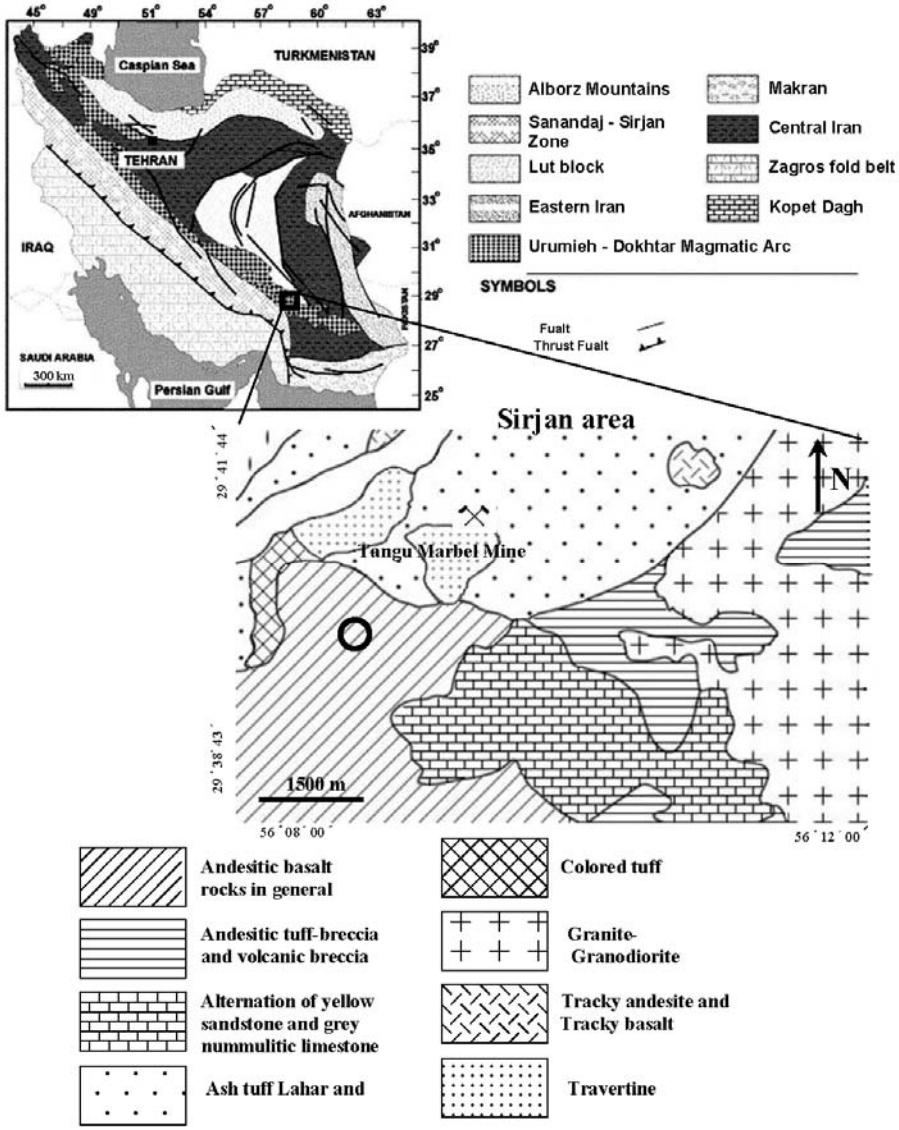


**Figure 1.** Simplified geological map of Iran (modified from STÖCKLIN & SETUDIEN, 1972) and simplified geological map the Sirjan area, Location of sample are given by circle (modified after geological map of Sirjan, Series 1: 100 000 (Geological Survey of Iran)).

the population density of crystals (n) is expressed as

$$n = n_o \exp(-L/G_t)$$

Where L is crystal size, G is growth rate; t is resident time and $n_o$ is the nucleation density. Thus on a standard CSD plot of crystal size versus ln (population density), the slope provides a measure of the growth rate and residence time of crystals in the magmatic system, and the intercept gives the nucleation density [18, 20].

Textural analytical methods generally follow those presented in Armienti *et al*. [2]. Prints of digital photograph were first prepared for quantitative crystal size distribution analyses. Then, the binary plagioclase image was acquired using the Adobe Illustrator CS program from a microscopic photograph of the thin section (Fig. 4). A list of rough area determinations of the crystals and total area investigation were obtained using the program Image J, a java version of the well-known program NIH Image. Following the calculation procedures described by Armienti *et al*. [2], a diagram of ln (population density) vs. crystal size was plotted (Fig. 6), defined as the number per unit volume and unit size, of given linear dimension L [18]. 603 crystals were detected in 30 $mm^2$ total areas measured. Throughout this report, "size" is the radius of the equivalent sphere reconstructed from the section of crystal.

**Table 1.** Representative analysis of plagioclase phenocrysts

| Crystal | SiO2 | Al2O3 | FeO | CaO | Na2O | K2O | TiO2 | Total | An* | Distance (μm)** |
|---|---|---|---|---|---|---|---|---|---|---|
| A | 55.842 | 26.656 | 0.424 | 9.910 | 5.755 | 0.517 | 0.047 | 99.151 | 45.37 | 0 |
| rim-core-rim | 53.554 | 28.962 | 0.468 | 12.364 | 4.625 | 0.353 | 0.045 | 100.370 | 57.22 | 71 |
| | 53.647 | 28.681 | 0.462 | 12.372 | 4.838 | 0.334 | 0.049 | 100.383 | 55.56 | 101 |
| | 49.504 | 31.075 | 0.503 | 15.099 | 3.114 | 0.177 | 0.023 | 99.494 | 70.29 | 341 |
| | 54.090 | 28.126 | 0.532 | 11.591 | 5.194 | 0.338 | 0.025 | 99.896 | 52.43 | 510 |
| | 54.108 | 28.685 | 0.506 | 11.979 | 4.593 | 0.299 | 0.024 | 100.195 | 56.77 | 795 |
| | 50.665 | 30.538 | 0.486 | 14.527 | 3.432 | 0.178 | 0.029 | 99.855 | 67.39 | 995 |
| | 54.316 | 28.464 | 0.472 | 11.640 | 5.079 | 0.394 | 0.051 | 100.416 | 53.7 | 1124 |
| | 53.888 | 28.870 | 0.472 | 12.051 | 5.190 | 0.307 | 0.020 | 100.798 | 54.57 | 1288 |
| | 56.919 | 26.749 | 0.398 | 9.890 | 5.637 | 0.532 | 0.010 | 100.135 | 46.11 | 1431 |
| | 56.396 | 26.687 | 0.634 | 10.612 | 4.978 | 0.522 | 0.033 | 99.861 | 46.93 | 1458 |
| B | 50.994 | 30.514 | 0.530 | 14.283 | 3.560 | 0.205 | 0.035 | 100.121 | 66.67 | 0 |
| core-rim | 52.655 | 29.963 | 0.479 | 13.386 | 4.119 | 0.225 | 0.025 | 100.851 | 62.6 | 77 |
| | 54.024 | 28.205 | 0.415 | 11.762 | 4.854 | 0.383 | 0.070 | 99.713 | 54.04 | 113 |
| | 53.494 | 28.958 | 0.501 | 12.576 | 4.486 | 0.262 | 0.055 | 100.333 | 58.1 | 134 |
| | 54.263 | 28.540 | 0.492 | 11.937 | 4.952 | 0.328 | 0.034 | 100.546 | 54.68 | 140 |
| | 55.549 | 27.917 | 0.555 | 10.745 | 5.563 | 0.423 | 0.031 | 100.782 | 49.95 | 159 |
| | 54.724 | 27.180 | 1.038 | 11.313 | 4.986 | 0.721 | 0.052 | 100.102 | 49.65 | 183 |
| | 55.627 | 27.737 | 0.533 | 10.940 | 5.536 | 0.412 | 0.011 | 100.794 | 49.62 | 277 |
| | 51.670 | 30.178 | 0.589 | 13.579 | 3.921 | 0.222 | 0.031 | 100.189 | 64.09 | 292 |
| C | 53.732 | 28.59 | 0.442 | 12.046 | 4.968 | 0.324 | 0.022 | 100.125 | 54.75 | 0 |
| core-rim | 54.045 | 27.684 | 0.678 | 11.612 | 5.109 | 0.367 | 0.022 | 99.637 | 51.52 | 114 |
| | 51.004 | 30.441 | 0.477 | 14.209 | 4.017 | 0.208 | 0.000 | 100.356 | 64.42 | 137 |
| | 55.128 | 27.444 | 0.426 | 11.029 | 6.098 | 0.406 | 0.046 | 100.577 | 46.31 | 163 |
| | 55.589 | 27.689 | 0.498 | 10.862 | 5.639 | 0.413 | 0.084 | 100.774 | 49.02 | 224 |
| | 53.054 | 29.107 | 0.418 | 12.640 | 4.213 | 0.302 | 0.019 | 99.753 | 59.62 | 298 |
| | 54.977 | 27.527 | 0.406 | 11.042 | 6.305 | 0.428 | 0.008 | 100.693 | 45.54 | 360 |
| | 51.786 | 30.107 | 0.657 | 13.770 | 3.882 | 0.231 | 0.015 | 100.448 | 64.04 | 399 |
| | 51.315 | 30.471 | 0.716 | 14.525 | 3.509 | 0.148 | 0.029 | 100.712 | 66.95 | 466 |

Oxide units in weight present, *anorthite content in mol%, **microns measured for phenocryst.

## Results and Discussion

### *Mineralogy of Plagioclase*

The most common crystalline phase in our samples is plagioclase (nearly 40%) that occurs primarily as isolated grains. These plagioclase crystals are subhedral to euhedral showing polysynthetic twinning. Based on texture and composition, plagioclase crystals falls into two groups of population. The most common population (>80%) consists of zoned plagioclase crystals characterized by resorption zones (Fig. 2a). The second group, less common population (<20%) is composed of grains with a coarsely sieved interior (Fig. 2b). This texture results from the presence of extensive network of interconnecting inclusions that pervades the crystals interior.

Electron microprobe analyses of zoned plagioclase grains show XAn (mol %) varies from 45.4 to 70.3 (Fig. 5). Therefore, they can chemically be classified predominantly as labradorite and less bytownite (Fig. 3). Variations of XAn plotted for two plagioclase grains

from core to rim and one grain from rim-core-rim show that the microprobe analyzed plagioclase grains have resorption zoning patterns (dissolution-reprecipitation textures) (Fig. 5). Plagioclase in Figure 5A shows an inner zone with relatively constant XAn of around 50, followed by an outward increase in XAn of around 70. Plagioclase crystals in Figure 5B and 5C show some irregular zoning with an overall decrease in XAn towards the rim of around 45. Although the plagioclase in Figure 5B does not display high An variations, plagioclase in Figure 5C demonstrates high An variations.

Zoning in plagioclase is described by changes in An-content, generally ranging from 1 to over 30 mol % An [9]. The variation of XAn (mol %) can be produced in general by two main factors: The first is the repeated changes in the crystallization conditions during crystal growth in a dynamic magma chamber. The second is repeated magma replenishing followed by compositional changes if mechanical and chemical mixing is sufficient [6]. Therefore, a gradient in temperature is expected in magma chambers, at least in the thermal/chemical boundary layer [19]. In addition, transfer of the crystals can occur along these gradients of periodic changes in temperature by convection in the water content, bulk composition, and to a less extent, pressure, depending on the extent of the convection [e.g. 23, 24, 27, 28, 29, 9].

Major resorption surfaces with oscillation patterns in plagioclase are mostly ascribed to changes in water content, temperature, melt composition and pressure, magma mixing and destabilization of the crystal-melt interface and a critical value of growth rate versus diffusion rate [e.g. 23, 28, 29, 9].

The principal controls on composition and stability plagioclase of in calc-alkaline magmas are melt $H_2O$ content and temperature [13, 27]. Increasing $H_2O$ a long with depression of the plagioclase liquidus causes the high An content of plagioclase in equilibrium with a melt to increase [13]. In a hydrous magma in small shallow chamber, plagioclase may dissolve by crystal settling or convection of magma that conveys phenocrysts through modest pressure gradients sufficient to change melt $H_2O$ content [27]. Rapid devolatilization during an eruption or influxes of $H_2O$ from hydrous magma is another agent of plagioclase dissolution [27].

Furthermore, the high An content outward of the dissolution surfaces may indicate a temperature increase. As temperature difference of only 5-10°C of a multicomponent melt in equilibrium with plagioclase is sufficient to cause resorption zones by diffusive dissolution of the crystal, therefore the rate and amount

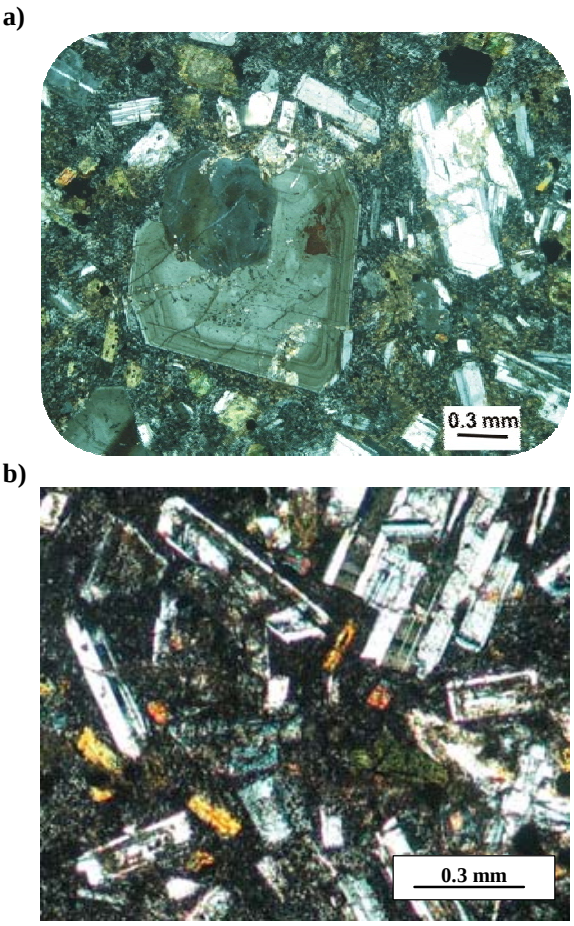


**Figure 2.** Photomicrographs showing typical texture of plagioclase crystals from Sirjan area. a) Sieve core crystal with zoned rim, this plagioclase has micrometer-scale inclusions of glass and minerals suggest a reaction between preexisting plagioclase and melt that overgrown by zoned plagioclase b) Plagioclase with resorption zone.

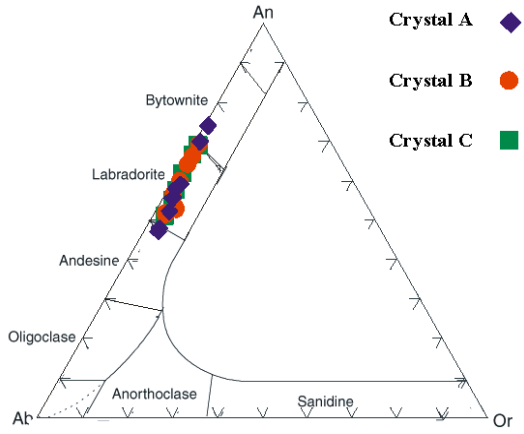


**Figure 3.** Compositions of zoned plagioclases and nomenclatures.

of dissolution correspond to the temperature increase [24,27].

The maximum difference in XAn is more than 20 mol% in our plagioclase crystals (Fig. 5). Ghiorso *et al*. [7] shows that if temperature varies by 10°C then the XAn value will change by 1 mol%. Therefore, the sample would require an uncommonly high change in temperature of 200°C if temperature by itself caused the change in XAn.

Furthermore, Ghiorso *et al*. [7] shows that if pressure varies by 1 kbar then the An value will change by 1.4 mol%. Longhi *et al*. [16] specifies that 1 kbar increase in pressure leads to a 1 mol% decrease in XAn, if pressure is the only variable. Therefore, the observed maximum change in XAn of 20 mol% would require an extraordinary high pressure change of about 20 kbar. Indeed, a huge chamber of some 50-60 km of vertical thickness would be required which seems unrealistic for calc-alkaline magmas in subduction zone settings. Hence, it is highly unlikely that the changes in XAn are due to pressure changes alone.

It is more plausible that a magma mixing process has caused the major resorption surfaces in plagioclase based on the above arguments.

The sieve textured cores in some plagioclase phenocrysts are overgrown by oscillatory zoned plagioclase (Fig. 2). The sieved core texture with abundant inclusions of minerals and glass (melt) suggest a reaction between early plagioclase and melt (Fig. 2) [30]. Plagioclase sieve cores may be produced by rapid decompression and degassing of plagioclase-saturated magma rising from deep to shallow depth [22, 14].

Regular depressurisation-degassing of hydrous magma can increase dissolution and change the composition [22, 14]. Madeleine *et al*. [17] shows that if the Fe/Al ratio increases in zoned crystals from core to rim then this indicates a degassing process in the environment of the magma chamber. In andesitic basalt of Sirjan area, there is no clear trend in the Fe/Al zonation from core to rim in various crystals. Hence, a degassing process cannot be clearly confirmed. However, our CSD results show that degassing that has occurred in the magma chamber and caused the formation of resorption zones and sieve cores in plagioclase phenocrysts (Fig. 6).

### *Analysis of CSD Data*

Nucleation and growth rates of crystals are controlled by the magnitude of the crystallisation driving force, which can be expressed thermally as undercooling or chemically as saturation. Change in intensive parameters, like temperature and $XH_2O$ in a fluid and pressure will change the driving forces for crystallisation [12]. Magma mixing, a very common process, can be an agent of change in the driving force, as many plutonic and volcanic rocks show plentiful evidence for mixing.

CSD graphs contain information on crystal growth rate and growth time. Assuming simple, linear crystal growth, the CSD will be straight line, the gradient of which is related to the crystal growth rate and the time that has elapsed during the crystallization. The semi-logarithmic CSD diagram of our sample shows a kinked line. The gently sloped part of the CSD has values of 4.3 for the intercept and -5.0 for the slope. The steeper sloped part has values of 8.1 for intercept and -12.6 for the slope, respectively (Fig. 6). Hence, a simple model based on a single population of crystals cannot be successfully applied. The kinked CSD plots can be the results of various complicated processes observed in following examples:

1- The CSDs examination of plagioclase crystals in Mount Etna has shown strongly curved CSDs, attributed to changing environments due to the abrupt changes in cooling rate during crystallization [1].

2- It has also been suggested that accumulation of crystals by gravity produces a curved CSD on a classical CSD diagram and gentler CSD slope shows that larger crystals descend faster than the smaller crystals [18].

3- Mixing of two magmas with non-collinear straight CSDs produces a concave up curved CSD [11]. The log-linear CSD dictates that each initial CSD dominates the slope of new CSD in the region where it has the highest population density regardless of the mixing ratios. Given that the two initial CSDs have significantly different slopes the final CSD turns out to be kinked, i.e., the larger size range of crystals has a gentler slope whereas smaller ones posses a steeper slope.

In our sample, considering the ubiquitous phenocrysts comprising generally resorbed and zoned plagioclase, the most likely interpretation of the CSD plot is that it reflects mixing of two magmas with

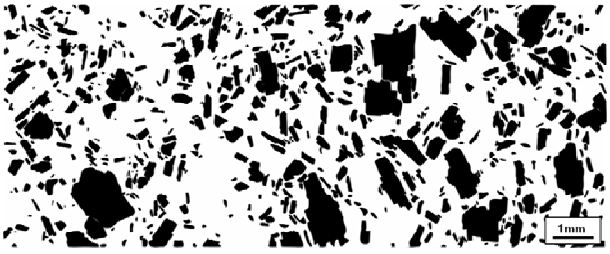


**Figure 4.** Digitized outlines of plagioclase from Sirjan area.

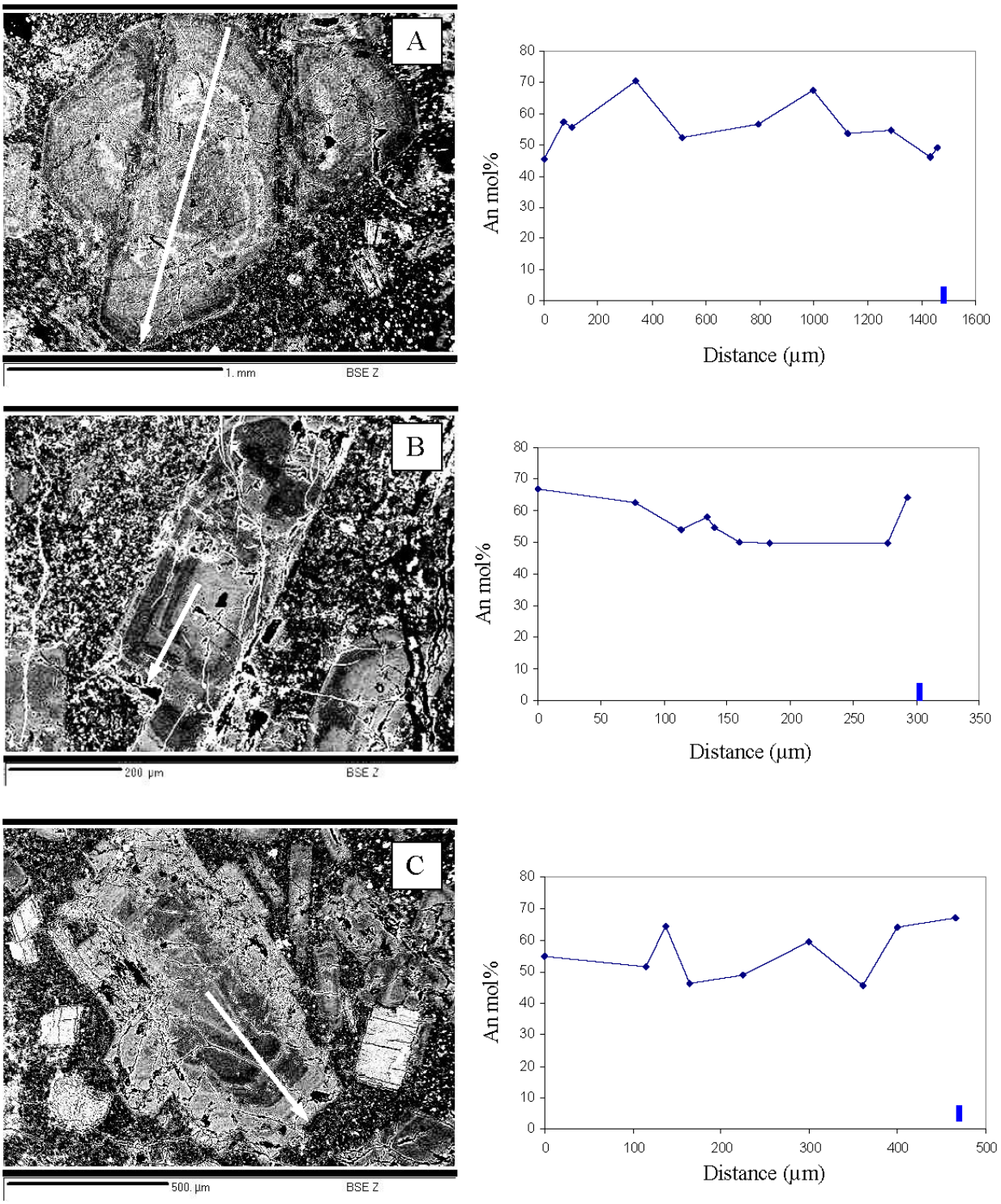


**Figure 5.** BSE images, grey light color show resoption surface contrast with clear gray zone. EPMA profiles of An content vs. distance are shown. Arrows indicate path of sampling transects for electron microprobe analyses (A) rim-core-rim for one plagioclase crystal, An (mole. %) change as repeated along analysis traverse in the crystal there is an inner zone with relatively constant XAn of around 50, followed by an outward increase in XAn to values of around 70; then there is some irregular zoning with an overall decrease in XAn towards the rim with values of around 45 and (B-C) core-rim for two plagioclase samples. (B) This plagioclase has not high An variation (C) plagioclase with high An (mol %) variation.

distinct initial CSDs as modeled by Higgins [11]. This suggests a delay in elemental diffusion in the entering magma has occurred during the growth of crystal face that emerges as a resorption zone. In fact, the kink in the curve indicates that the larger crystals start to interact with the linear region representing the simple population of smaller crystals [11].

Furthermore, the CSD plot shows peaks in the size distribution that indicate bursts in nucleation caused by degassing and undegassing during the mixing, which strongly affects nucleation and growths rate (Fig. 6) [1]. The degassing process has been explained as being due to inputs of volatile-rich magma into the host magma [22, 14]. Plagioclase, growing in equilibrium with the host magma, can be admixed in the magma of which high $H_2O$ content and high temperature induces plagioclase resorption. The degree of undercooling experienced by the replenishing magma is a function of thermal ($\Delta T$) and compositional contrast ($\Delta C$) between the replenishing and host magmas before mixing, and the volume of replenishing magma [3]. In this scenario, the sieve-texture cores of phenocrysts are interpreted to reflect gradual degassing by rapid decompression from high pressure which may be expected for an intrusive magma prior to intrusion.

Some plagioclase phenocrysts are not enclosed by resorption zones. The presence of both resorbed and non-resorbed plagioclase in association with replenishment events may be the result of mixing [e.g. 6].

Moreover, the CSD plot shows a dog-leg where a small offset separates two regions of the same gradient. The dog-leg portion indicates high abundance of small size crystals and could emerge due to a transient increase in growth rate or quenching procedure at various rates (Fig. 6) [1,2].

The concluding remarks that can be deduced from this study are as follow:

Chemical and CSD analysis make possible to distinguish a significant change in magmatic process. In this case, we integrated micrometer-scale analyses on distinct plagioclase textures which record phenocryst exchange events between intruded magma and host magma. Furthermore, the kink in the crystal population could result from a mixed population of crystals. The CSD method also clearly shows a degassing process in magma chamber. This finding demonstrates that magma mixing is principal mechanism for the origin of the textural and mineralogical diversity that is diagnostic of Sirjan magmas. However, further isotope data and petrogenesis study in future are needed to confirm our CSD study which is the first attempt to approach the petrology of the volcanic rocks in Iran.

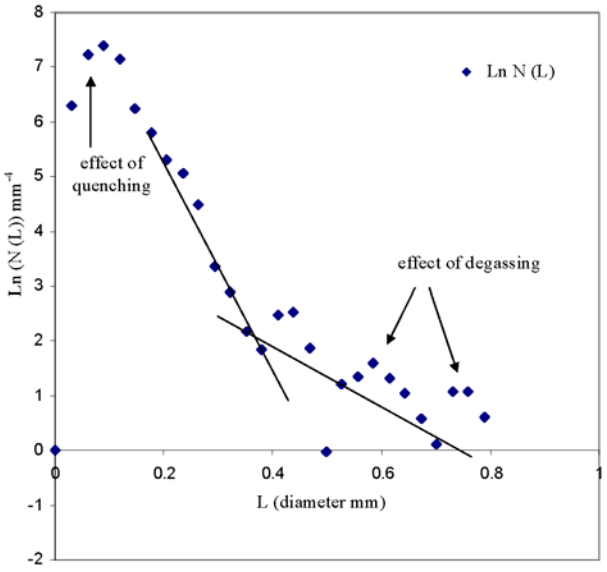


**Figure 6.** Selected plagioclase crystal size distribution from andesitic basalt sample from Sirjan. Data are shown in semi-logarithmic diagram *vs.* the size of the grain. Size is assumed equal to the radius of the circle whose area is equivalent to the area of the mineral in the section. Equivalent radii in mm. Number densities n(L) in mm-4. Kinked CSD reflects a sequence of two nucleation events. Additionally, CSD shows effect of degassing and quenching on diagram.

## Acknowledgements

This work has been performed by financial support of Research Deputy of Tarbiat Moallem University, Tehran.

## References

1. Armienti P., Pareschi M.T., Innocenti F. and Pompilio M. Effects of magma storage and ascent on the kinetics of crystal growth. The case of 1991-93 Mt. Etna eruption. *Contributions to Mineralogy and Petrology*, **115**, 402-414 (1994).
2. Armienti P., Francalanci L. and Landi P. Textural effects of steady state behaviour of the Stromboli feeding system. *Journal of Volcanology and Geotermal Research*, **160**, 86-98 (2007).
3. Bacon C. R. Magmatic inclusions in silicic and intermediate volcanic rocks. *Journal of Geophysical Research*, **91**, 6091-6112 (1986).
4. Berberian M. 1983 Generalized tectonic map of Iran. *In*: BERBERIAN, M. (*Eds*), Continental Deformation in the Iranian Plateau. Geological Survey of Iran, Report No. 52.
5. Berberian M. and King G.C.P. Towards a paleogeography and tectonic evolution of Iran. *Canadian Journal of Earth Sciences*, **18**, 210-265 (1981).
6. Browne B. L., Eichelberger J. C., Patino L. C., Vogle T.

A., Uto K. and Hoshizumi H. Magma mingling as indicated by texture and Sr/Ba ratios of plagioclase phenocrysts from Unzen volcano, SW Japan. *Journal of Volcanology and Geotermal Research*, **154**, 103-116 (2006).

7. Ghiorso M.S., Carmichael I.S.E., Rivers M.L. and Sack R.O. The Gibbs free energy of mixing of natural silicate liquids: An expanded regular solution approximation for the calculation of magmatic intensive variables. *Contributions to Mineralogy and Petrology*, **84**, 107-145 (1983).
8. Ginibre C., Worner G. and Kronz A. Minor- and trace-element zoning in plagioclase: implications for magma chamber processes at Parinacota volcano, northern Chile. *Contributions to Mineralogy and Petrology*, **143**, 300-315 (2002a).
9. Ginibre C., Kronz A. and Worner G. High-resolution quantitative imaging of plagioclase composition using accumulated backscattered electron images: new constraints on oscillatory zoning. *Contributions to Mineralogy and Petrology*, **142**, 436-448 (2002b).
10. Halama R., Waight T. and Markl G. Geochemical and isotopic zoning patterns of plagioclase megacrysts in gabbroic dykes from the Gardar Province, South Greenland: implications for crystallization processes in anorthositic magmas. *Contributions to Mineralogy and Petrology*, **144**, 109-127 (2002).
11. Higgins M.D. Magma dynamics beneath Kameni volcano, Greece, as revealed by crystal size and shape measurements. *Journal of Volcanology and Geothermal Research*, **70**, 37-48 (1996).
12. Higgins M. D. and Roberge J. Three magmatic components in the 1973 eruption of Eldfell volcano, Iceland: Evidence from plagioclase crystal size distribution (CSD) and geochemistry. *Journal of Volcanology and Geotermal Research*, **161**, 247-260 (2007).
13. Housh T.B. and Luhr J.F. Plagioclase-melt equilibria in hydrous systems. *American Mineralogist*, **76**, 477-492 (1991).
14. Landi P., Métrich N., Bertagnini A. and ROSI, M. Dynamics of magma mixing and degassing recorded in plagioclase at Stromboli (Aeolian Archipelago Italy). *Contributions to Mineralogy and Petrology*, **147**, 213-237 (2004).
15. Lofgren G. E. Experimental studies on the dynamic crystallization of silicate melts. *In*: HARGRAVES R. B. (*Ed.*) Physics of magmatic processes, pp. 487-551. Princeton University Press, Princeton, New Jersey (1980).
16. Longhi J., Fram M. S., Auwera J. V. and Montieth J. N. Pressure effects, kinetics, and rheology of anorthositic and related magmas. *American Mineralogist*, **78**, 1016-1030 (1993).
17. Madeleine C. S., Humphreys J., Blundy D., Stephan R. and Sparks J. Magma evolution and open-system processes at Shiveluch Volcano: insight from phenocrysts zoning. *Journal of Petrology*, **47**, 2303-2334 (2006).
18. Marsh B.D. Crystal size distribution (CSD) in rocks and the kinetics and dynamics of crystallization I. Theory. *Contributions to Mineralogy and Petrology*, **99**, 277-291 (1988).
19. Marsh B.D. Magma chambers. *Annual Reviews of Earth and Planetary Science*, **17**, 439-474 (1989).
20. Marsh B.D. On the interpretation of crystal size distributions in magmatic systems. *Journal of Petrology*, **39**, 553-599 (1998).
21. Mohajjel M., Fergusson C.L. and Sahandi M.R. Cretaceous-Tertiary convergence and continental collision, Sanandaj-Sirjan Zone, Western Iran. *Journal of Asian Earth Sciences*, **21**, 397-112 (2003).
22. Nelson S.T. and Montana A. Sieve-textured plagioclase in volcanic rocks produced by rapid decompression. *American Mineralogist*, **77**, 1242-1249 (1992).
23. Nixon G.T. and Pearce T.H. Laser-interferometry study of oscillatory zoning in plagioclase: The record of magma mixing and phe-nocryst recycling in calc-alkaline magma chanjbers, Iztaccihuatl volcano, Mexico. *American Mineralogist*, **72**, 1144-1162 (1987).
24. Pearce T.H. and Kolisnik A.M. Observations of plagioclase zoning using interference imaging. *Earth-Science Reviews*, **29**, 9-26 (1990).
25. Perugini D., Poli G., and Valentini L. Strange attractors in plagioclase oscillatory zoning: petrological implications. *Contributions to Mineralogy and Petrology*, **149**, 482-497 (2005).
26. Ricou L.E., Braud J. and Brunn J.A. 1977 Le Zagros. *Memoire Societe Geologique de France*, **8**, 33-52.
27. Singer B. S., Dungan M. A. and Layne G. D. Textures and Sr, Ba, Mg, Fe, K, and Ti compositional profiles in volcanic plagioclase: clues to the dynamics of calc-alkaline magma chambers. *Americam Mineralogist*, **80**, 776-798 (1995).
28. Tepley F. J. III, Davidson J. P. and Clynne M. A. Magmatic interactions as recorded in plagioclase phenocrysts of Chaos Crags, Lassen Volcanic Center, California. *Journal of Petrology*, **40**, 787-806 (1999).
29. Tepley F. J. III, Davidson J. P., Tilling R. I. and Arth J. G. Magma mixing, recharge and eruption histories recorded in plagioclase phenocrysts from El Chichon Volcano, Mexico. *Journal of Petrology*, **41**, 1397-1411 (2000).
30. Tsuchiyama, A. Dissolution kinetics of plagioclase in the melt of the system diopside-albite-anorthite, and the origin of dusty plagioclase in andesites. *Contributions to Mineralogy and Petrology*, **89**, 1-16 (1985).